

**Movement ecology of swordfish (*Xiphias gladius*) in the
northwestern Pacific Ocean using electronic tags and stable
isotope analysis**

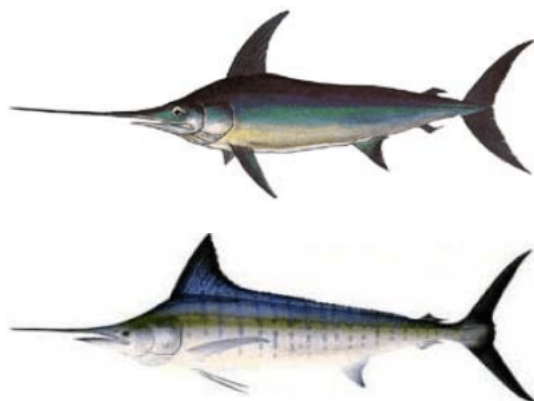
Wei-Chuan Chiang^{1*}, Shian-Jhong Lin^{1,2}, Qi-Xuan Chang¹, Ching-Tsun Chang¹, Michael K. Musyl³,
Yuan-Shing Ho¹

1. Eastern Marine Biology Research Center, Fisheries Research Institute, Taiwan

2. Department of Environmental Biology and Fishery Science, National Taiwan Ocean
University, Taiwan

3. Pelagic Research Group LLC, USA Authors name*

Email: wcchiang@mail.tfrin.go.tw



Abstract

Swordfish (*Xiphias gladius*) is a highly migratory apex predator distributed from tropical to temperate oceans. The objective of this research is to use a combination of stable isotope analysis (SIA) and electronic tagging experiments to identify swordfish trophic position and movement behavior in eastern Taiwan. In total, 165 swordfish muscle samples (59-210 cm eye-orbit fork length, EFL) were examined for trophic position and population dynamics. $\delta^{15}\text{N}$ and $\delta^{13}\text{C}$ values for swordfish ranged from 7.9 to 14.3‰ and -18.9 to -15.4‰, respectively, and were all positively correlated with size. Mid-water prey species were major food resources for swordfish (e.g., Cephalopoda and Bramidae spp.) diet which was highly diverse. Three swordfish were tagged pop-up satellite archival tags (PSATs) and tags remain affixed from 14 and 229 days-at-liberty. From the tagging location in eastern Taiwan, pop-up locations ranged northwards to the East China Sea, southwest to the South China Sea and the another to the southeast off the Philippines. The total linear displacements were from 631 to 1,605 km from deployment to pop-up locations and the fish demonstrated pronounced diel vertical movement patterns reaching daytime of depths >400 m (15–20°C) and occupying the surface mixed layer <100 m at nighttime (occasionally experiencing temperatures of 32.9°C). Distributions of time spent at depth were significantly different between daytime and nighttime where fish displayed a regular crepuscular pattern of ascending into the surface layer at dusk and remaining there until the following dawn where the fish descended past the mixed-layer depth. This pattern has been reported previously and suggests swordfish follow the diel vertical migrations of prey organisms comprising the deep sound scattering layer to exploit them effectively as a resource. Because of its unique physiological and morphological adaptations (such as vascular counter current heat exchangers), swordfish can search for food resources more effectively in cooler temperatures and exploit more resources of the water column than other fishes.

Keywords: deep sound scattering layer, diel patterns, migration, trophic dynamics

Introduction

Swordfish (*Xiphias gladius*) is a cosmopolitan species found in tropical and temperate waters of all the oceans (Nakamura 1985). They are distributed between ~48°N and 45°S (Palko et al. 1981, Ichinokawa and Brodziak 2010). Mainly because of its evolved ability to withstand water temperature fluctuations from ~6 to 26°C (Carey and Robinson 1981), it is one of the mostly widely distributed pelagic species; both horizontally and vertically. Based on genetic studies, swordfish in the Indo-Pacific region can be pooled into three stocks: (1) northern Madagascar, (2) Bay of Bengal, and (3) Indian Ocean and western Pacific (Lu et al. 2006). Swordfish are an economically important species, primarily caught as bycatch in commercial tuna longline fisheries, such as the Japanese and Taiwanese longline fleets in the western and central Pacific Ocean (Su et al. 2020). Understanding short- and long-term movement patterns and habitat preferences is essential for robust assessments and developing management plans (Brill and Lutcavage 2001).

Defining population connectivity and migratory routes for species is essential to differentiate discrete populations for comprehending their population dynamics and life-history strategies for management (Pekarsky et al. 2015, Zhu et al. 2020). Certain “intrinsic tracers” in tissues can provide retrospective information on both the movements and diet of sampled individuals (Madigan et al. 2015). Isotope ratios of carbon ($\delta^{13}\text{C}$) and nitrogen ($\delta^{15}\text{N}$) have been the most commonly used intrinsic tracers in pelagic marine faunal studies (Madigan et al. 2016).

Multiple techniques have been employed to describe the geospatial movements of marine animals and these advances provided unprecedented ecological insights by connecting animal movements to measures of their physiology and environment (Block et al. 2011, Hussey et al. 2015). Pop-up satellite archival tag (PSAT) technology is an established fisheries-independent tool to monitor ambient depth (pressure), temperature, and light levels on tags attached to animals to chronicle both horizontal and vertical movement patterns (Block et al. 1998; Lin et al. 2020a). PSATs can offer many benefits to study vertical dive behaviors, as well as providing information on migration routes, possible spawning areas, thermal habitat, exchange rates between areas and post-release mortality (Hoolihan et al. 2011, Chiang et al. 2015, Musyl and Gilman 2019, Chang et al. 2020, Griffiths 2020, Madigan et al. 2020). The objective of this research is to use a combination of stable isotope analysis (SIA), stomach contents analysis (SCA) and electronic tagging experiments to identify swordfish trophic position and movement behavior in eastern Taiwan.

Methods and materials

Field sampling and sample processing

Swordfish muscle samples were collected from fish captured off eastern Taiwan during May 2018 to March 2020 (Fig. 1). Swordfish were caught by commercial longline fisheries and landed at Shinkang fish market (southeastern Taiwan). Eye-to-fork length (EFL; posterior margin of bony orbit to the distal end of the central ray of the caudal fin; nearest cm) was measured using stainless steel calipers for each swordfish. A total of 169 muscle tissues were sampled (EFL: 59–210 cm). White muscle samples were taken from the posterior hypaxial region, ~10 cm beneath the skin, and were frozen at -80°C until processing. Prior to isotopic analysis, the muscle samples were rinsed with distilled water and freeze-dried for 48 h.

Stomach content analysis

A total of 51 swordfish stomachs (EFL: 70–220 cm) collected at Shinkang fish market were used for SCA. Swordfish were caught by inshore commercial fisheries and refrigerated immediately with ice on board to keep freshness of body. We obtained these swordfish samples after competitive bidding and stomachs were removed for analysis at the laboratory. Each stomach was cut open, and contents were washed through a 1-mm mesh size sieve. Identification on taxa was carried out to the lowest possible taxonomic level (Froese and Pauly 2020). Wet weight and fork length (FL) of prey items were measured to the nearest g and cm, respectively.

Diet was analyzed by calculating three diet indices for each prey taxon: (1) percentage by number (%N), (2) frequency of occurrence (%FO), and (3) percentage by wet weight (%W). For quantitative analysis of gastric contents, the index of relative importance (IRI) was calculated to represent the most important prey items (Cortés 1997) as a percentage relative to the diet composition by the following equation:

$$\text{IRI} = (\%W + \%N) \times \%FO$$

To readily allow comparison among prey items, IRI was standardized to %IRI for each prey item (Cortés 1997).

Stable isotope analysis

After freeze-drying, muscle samples were ground to a homogeneous powder. Approximately 0.5 to 0.7 mg of homogenate was weighed into ultra-clean tin capsules for $\delta^{13}\text{C}$ and $\delta^{15}\text{N}$ analyses (Davenport and Bax 2002). Samples were combusted in an elemental analyzer (Flash EA-2000, Thermo-Finnigan;

www.thermoscientific.com) to produce CO₂ and N₂, which flowed through a Gas Chromatography (GC) column for separation and then into a mass spectrometer (Thermo-Delta V Advantage) for determining isotopic composition. The δ¹⁵N values were standardized by air and the δ¹³C were standardized by USGS-40. The stable isotope values were expressed in standard ‰ notation using international standards (Vienna Pee Dee Belemnite limestone (V-PDB) for carbon and atmospheric N₂ for nitrogen).

According to a previous reproductive study (Wang et al. 2003), 50% of swordfish reached sexual maturity at ~145 cm EFL (~168 cm lower jaw to fork length) and stable isotope values were also reported to significantly shift over the size range 120–170 cm (LJFL). Therefore, to examine whether there was a shift in diet between different life stages, we pooled swordfish samples into three groups; Class I (<120 cm), Class II (121–170 cm) and Class III (>170 cm, EFL).

PSAT tagging

Swordfish were captured off eastern Taiwan during 2016 to 2018 between 22.76°N to 23.33°N and 122.13°E to 122.64 °E (Fig. 1) using commercial tuna longline gear (i.e., four hooks between floats, green chemical light sticks attached above the hooks baited with squid (*Loglio* spp.) and Pacific saury (*Cololabis saira*). Three swordfish (~60–180 kg, ~145–210 cm EFL)(Wang et al. 2006) in good condition were selected to affix PSATs and tags were placed at the base of dorsal fin between spaces of the interneural and neural spines using a ~2 m tagging pole. PSAT tag heads were made of surgical grade nylon and augmented with opposable flopper blades (Musyl et al. 2011b). The tether was made of ~123 kg fluorocarbon with stainless steel crimps matching the diameter of the line and a stainless steel ball bearing (Sampo no. 6, Barneveld, NY, USA) was placed ~10 cm from the tag head to reduce torque and precession.

We used two models of PSATs; one PTT-100 and two X-tags all from Microwave Telemetry (MT, Columbia, MD, USA). PSATs were tested with attached tether and tag head to ensure it was positively buoyant as this would allow discrimination of a shed tag from a dead sinking animal with the tag attached. Before tagging, the tag head, tethers and stainless applicator tip on the tagging pole were disinfected with alcohol and a bacitracin-neomycin ointment was applied before tagging to prevent wound ulceration and infection. The captured swordfish were slowly retrieved to alleviate possible barotrauma and the fish did not appear to be injured from the process of capture, tag and release. Tagging location (GPS) was recorded and body mass of the swordfish was estimated by the captain.

PSAT programming

The PSATs were programmed to release 12 (PTT-100) and 8 months (X-tag) after release. The PTT-100 was ~41 mm × 166 mm (with the antenna protruding to 171 mm), weighed ~65 g and was coated with antifouling paint. The PTT-100 PSAT had variable memory capability and acquired temperature and pressure readings every 15 min for the first 4 months of the deployment, collected data at 30 min intervals from 4 to 8 months, and at hourly intervals for deployments >8 months. The X-Tags were covered in antifouling paint and were 120 × 32 mm with the antenna protruding 185 mm, and weighed 40 g in air. PSATs had a depth range of 0~1,250 m (resolution 0.34~5.4 m), and a temperature range of -4~40°C (resolution 0.16-0.23°C).

PSATs were equipped with automatic release and fail-safe emergency depth release features whereby the procedure was initiated when a constant depth was detected or if the tag descended below the emergency depth threshold (1,250 m) (Musyl et al. 2011b). On the programmed date or if the release mechanism is initiated; the tag releases, surfaces, and uploads archived data to the Argos constellation of polar orbiting satellites.

Geolocation and time at depth/temperature

We applied an (unscented) Kalman filter, augmented with sea surface temperature (SST) to calculate most probable tracks (MPTs) from the raw, light-based geolocations (Lam et al. 2008, Lam et al. 2010). Pop-up locations were estimated by Doppler shift with Argos messages with location classes of 1 or higher and linear displacements from deployment to pop-up locations were determined using the Great Circle Distance. Time-at-depth and time-at-temperature data were aggregated into 50 m and 1°C bins, respectively and were separated into daytime and nighttime periods by calculating times of local sunrise and sunset time (<http://aa.usno.navy.mil/>).

Thermal habitat distributions were expressed as differences (Δ SST) from average daily SST estimates (Brill et al. 1993, Musyl et al. 2011a). Vertical swimming speeds for ascents and descents were calculated from the directional changes in swimming patterns by examining the time series data. The correlation of nighttime depth and lunar illumination (uncorrected for cloud cover; <http://aa.usno.navy.mil/>) was examined. One sample Kolmogorov-Smirnov tests indicated daytime and nighttime distributions of depth, temperature and vertical speeds were not normally distributed. As a result, we used non-parametric two-sample Kolmogorov-Smirnov tests and Mann-Whitney W-tests to compare daytime and nighttime diving behaviours (Zar 2010). Simple linear regression

and Kruskal-Wallis one-way ANOVAs were used for the SIA (Zar 2010).

Results and Discussion

Feeding ecology

In total, six prey species were identified comprising four teleost species, two cephalopod species and one shrimp species (Table 1). Mid-waters prey species were major food items for swordfish (e.g., Cephalopoda and Bramidae spp.). According to the %IRI, the most important prey items were unidentified fish (49.2%), followed by pomfret (Bramidae spp) (23.3%), unidentified cephalopod (16.9%), diamond squid (*Thysanoteuthis rhombus*) (9.9%) and shrimp (0.6%). The analysis of %IRI by size classes showed that there was preferential prey compositions for different sized fish for any given size class. From the values of this index, cephalopods and fishes were main prey for the three size classes considered (Fig. 2).

Stable isotope values of $\delta^{15}\text{N}$ and $\delta^{13}\text{C}$ for swordfish size classes are given in Table 2. Body size of swordfish from eastern Taiwan was significantly and positively correlated with $\delta^{15}\text{N}$ and $\delta^{13}\text{C}$ values (linear regression; $p < 0.05$) (Fig. 3). Moreover, we found $\delta^{15}\text{N}$ values were significantly higher in Class III compared to Class II and Class I (ANOVA; $F_{2,165}=3.19$, $p < 0.05$) while $\delta^{13}\text{C}$ values were not significantly different across swordfish size classes (ANOVA; $p > 0.05$).

Diving characteristics

PSATs popped-up prematurely after 15 to 229 days-at-liberty (Fig. 1; Table 3). Based on the MPTs, SWO#143509 undertook a southeasterly course of ~738 km east of the Philippines and SWO#45922 underwent a southwestern course of ~1,605 km to the South China Sea. SWO#45924 undertook a northwards course ~392 km to the East China Sea (Fig. 1).

Vertical movements extended to 915 m and ambient temperatures ranged from 4.5 to 32.9°C (Table 4). Daytime and nighttime diving patterns indicated clear and significantly different diel patterns. Mean depth (\pm SD) and ambient temperatures experienced during daytime and nighttime were 419 ± 173 m, $12.9 \pm 5.5^\circ\text{C}$ and 106 ± 101 m, $23.4 \pm 3.9^\circ\text{C}$, respectively (Table 4). Figure 4 displays remarkably consistent patterns in diel vertical movements with pronounced crepuscular transitions. At dawn, swordfish descended to depths generally below 500 m but made regular excursions to ~100 m into the warmer mixed-layer and at dusk, ascended into the surface layer and remained there until the following dawn. The percentage time spent at depth and temperature during daytime indicated swordfish tuna spent >50% of time at 400 to 500 m and spent >60% of

time <200 m (Fig. 5). Given the routes taken by each fish (Fig. 1), based on temperature-depth profiles, the bottom of the mixed-layer appears to be from ~150 - 200 m (Fig. 6). The Delta T analysis indicated daytime and nighttime vertical movements were limited by temperature changes of $\leq 18^{\circ}$ and $\leq 6^{\circ}\text{C}$, respectively (Fig. 7).

Temperature, salinity and oxygen profiles from CTD casts of the tagging area off eastern Taiwan indicated the mixed-layer was at ~100 m at ~25 °C, and the thermocline extended beyond 400 m at temperatures <10°C. The salinities from the surface to 200 m were 34.3 - 34.8 ‰, and dissolved oxygen from the surface to 150 m was 5.5 - 6.7 mg l⁻¹, with an extended oxycline to ~1,000 m where concentrations were 5.5 - 2.4 mg l⁻¹ (Lin et al. 2020b). Dissolved oxygen did not appear to be limiting for swordfish.

Movement ecology

We documented temporal-spatial behavior and vertical habitat use of the first PSAT tagged swordfish in eastern Taiwan. Movement and habitat characteristics are essential for understanding the ecology of this species and should be incorporated into stock assessment models to evaluate vulnerability to various fishing gears (Hinton and Nakano 1996, Brill and Lutcavage 2001). The diel activity patterns exhibited by swordfish reported herein were similar to what other researchers have reported (Dewar et al. 2011) and matches the general behavior of bigeye tuna (Musyl et al. 2003, Matsumoto et al. 2013, Lam et al. 2014, Schaefer et al. 2015, Lin et al. 2020b) and some pelagic sharks (Musyl et al. 2011a) to the extent allowed by their respective physiological tolerances and limitations.

Swordfish displayed characteristic W-shaped vertical movement patterns during daytime and nighttime (Fig. 4). The fish descended below the thermocline and then returned to the mixed layer and stayed mostly near or in the thermocline during daytime and at shallower depths during nighttime; mostly in the mixed-layer. Dawn and dusk are clearly the transition points for initiating diel vertical movements. SWO #143509 exhibited clear correlation between average night-time depth and lunar illumination ($r^2 = 0.539$, $p < 0.001$) where the fish occupied mean deeper night-time depths during the full moon and shallower depths during the new moon (Fig. 8).

The W-shaped movement patterns displayed in swordfish during daytime are an optimal search strategy to increase prey encounters (Sims et al. 2008). The W-shaped movement pattern involves rapid directional changes presumably increasing prey encounter rates without extensively increasing linear travel

distance (Horodysky et al. 2007). These behaviors have been considered a foraging strategy for many pelagic fishes and sharks (Musyl et al. 2003, Sims et al. 2005, Gleiss et al. 2019).

Abid et al. (2018) indicated swordfish diet composition varied significantly among season and significant correlation was found between the body length of predators and prey sizes. Because of its unique physiological and morphological adaptations (such as vascular counter current heat exchangers), swordfish can maintain their body temperature on an ephemeral basis below the thermocline. This foraging adaptation allows them to mirror the diel migration of mesopelagic fishes and cephalopods to exploit them effectively as a resource as indicated by our stomach contents analysis and SIA results.

Lastly, our meta-analysis suggests a significant trend of deep diving correlated with body size (Fig. 9). This finding was similar to the meta-analysis of Lin et al. (2020b) which suggested thermal inertia may allow larger tuna to undertake longer and deeper excursions than smaller bigeye tuna. Several studies on vertical movements in bigeye tuna in the Pacific and Atlantic reported significant differences in vertical diving behaviour that correlated with fish size (Dagorn et al. 2000, Musyl et al. 2003, Arrizabalaga et al. 2008, Lam et al. 2014, Hino et al. 2020). Our initial study suggests that future SCA and SIA studies on swordfish are required to better understand size-specific trophic dynamics. Moreover, contemporaneously collected data on environmental factors would better define the temporal and spatial scales of swordfish distribution and habitat. Lastly, spatially explicit, fisheries-independent information (e.g., tagging experiments) in the high-catch areas will be required to better understand fishery interactions.

Acknowledgements

We thank crew members of the tuna longline vessel *FV Shing-Chan Fa* and *Nan-Shin* Captains Chen, I-Wei and Jenq, Jenq-Ai for their skill catching swordfish. This study was funded by the Fisheries Research Institute, Council of Agriculture, Taiwan (grant nos. 107AS-11.1.2-A1, 108AS-11.1.2-A1 and 108AS-1.2.1-A2).

References

- Arrizabalaga, H., J. G. Pereira, F. Royer, B. Galuardi, N. GoÑI, I. Artetxe, I. Arregi, and M. Lutcavage. 2008. Bigeye tuna (*Thunnus obesus*) vertical movements in the Azores Islands determined with pop-up satellite archival tags. *Fisheries Oceanography* **17**:74-83.
- Block, B. A., H. Dewar, C. Farwell, and E. D. Prince. 1998. A new satellite

- technology for tracking the movements of Atlantic bluefin tuna. *Proceedings of the National Academy of Sciences* **95**:9384-9389.
- Block, B. A., I. D. Jonsen, S. J. Jorgensen, A. J. Winship, S. A. Shaffer, S. J. Bograd, E. L. Hazen, D. G. Foley, G. A. Breed, A. L. Harrison, J. E. Ganong, A. Swithenbank, M. Castleton, H. Dewar, B. R. Mate, G. L. Shillinger, K. M. Schaefer, S. R. Benson, M. J. Weise, R. W. Henry, and D. P. Costa. 2011. Tracking apex marine predator movements in a dynamic ocean. *Nature* **475**:86-90.
- Brill, R. W., and M. E. Lutcavage. 2001. Understanding environmental influences on movements and depth distributions of tunas and billfishes can significantly improve population assessments. *American Fisheries Society Symposium* **25**:179-198.
- Brill, R. W., D. B. Holts, R. K. C. Chang, S. Sullivan, H. Dewar, and F. G. Carey. 1993. Vertical and horizontal movements of striped marlin (*Tetrapturus audax*) near the Hawaiian Islands, determined by ultrasonic telemetry, with simultaneous measurement of oceanic currents. *Marine Biology* **117**:567-574.
- Carey, F. G., and B. H. Robinson. 1981. Daily patterns in the activities of swordfish, *Xiphias gladius*, observed by acoustic telemetry. *Fishery Bulletin* **79**:277-292.
- Chang, C. T., S. J. Lin, W. C. Chiang, M. K. Musyl, C. H. Lam, H. H. Hsu, Y. C. Chang, Y. S. Ho, and C. T. Tseng. 2020. Horizontal and vertical movement patterns of sunfish off eastern Taiwan. *Deep Sea Research Part II: Topical Studies in Oceanography* **175**:104683.
- Chiang, W. C., M. K. Musyl, C. L. Sun, G. DiNardo, H. M. Hung, H. C. Lin, S. C. Chen, S. Z. Yeh, W. Y. Chen, and C. L. Kuo. 2015. Seasonal movements and diving behaviour of black marlin (*Istiompax indica*) in the northwestern Pacific Ocean. *Fisheries Research* **166**:92-102.
- Cortés, E. 1997. A critical review of methods of studying fish feeding based on analysis of stomach contents: application to elasmobranch fishes. *Canadian Journal of Fisheries and Aquatic Sciences* **54**:726-738.
- Dagorn, L., P. Bach, and E. Jossé. 2000. Movement patterns of large bigeye tuna (*Thunnus obesus*) in the open ocean determined using ultrasonic telemetry. *Marine Biology* **136**:361-371.
- Davenport, S. R., and N. J. Bax. 2002. A trophic study of a marine ecosystem off southeastern Australia using stable isotopes of carbon and nitrogen. *Canadian Journal of Fisheries and Aquatic Sciences* **59**:514-530.
- Dewar, H., E. D. Prince, M. K. Musyl, R. W. Brill, C. Sepulveda, J. Luo, D. Foley, E. S. Orbesen, M. L. Domeier, N. Nasby-Lucas, D. Snodgrass, R. Michael Laurs, J. P. Hoolihan, B. A. Block, and L. M. McNaughton. 2011. Movements and

- behaviors of swordfish in the Atlantic and Pacific Oceans examined using pop-up satellite archival tags. *Fisheries Oceanography* **20**:219-241.
- Froese, R., and D. Pauly. 2020. FishBase. World Wide Web electronic publication. www.fishbase.org, version (12/2020).
- Gleiss, A. C., R. J. Schallert, J. J. Dale, S. G. Wilson, and B. A. Block. 2019. Direct measurement of swimming and diving kinematics of giant Atlantic bluefin tuna (*Thunnus thynnus*). *Royal Society Open Science* **6**:190203.
- Griffiths, S. P. 2020. Restricted vertical and cross-shelf movements of longtail tuna (*Thunnus tonggol*) as determined by pop-up satellite archival tags. *Marine Biology* **167**. 117. <https://doi.org/10.1007/s00227-020-03733-7>
- Hino, H., T. Kitagawa, T. Matsumoto, Y. Aoki, and S. Kimura. 2020. Development of behavioral and physiological thermoregulatory mechanisms with body size in juvenile bigeye tuna *Thunnus obesus*. *Fisheries Oceanography*. <https://doi.org/10.1111/fog.12515>
- Hinton, M. G., and H. Nakano. 1996. Standardizing catch and effort statistics using physiological, ecological, or behavioral constraints and environmental data, with an application to blue marlin (*Makaira nigricans*) catch and effort data from Japanese longline fisheries in the Pacific. *Inter-Am. Trop. Tuna Comm. Bull.* **21**:171-200.
- Hoolihan, J. P., J. Luo, F. J. Abascal, S. E. Campana, G. De Metrio, H. Dewar, M. L. Domeier, L. A. Howey, M. E. Lutcavage, M. K. Musyl, J. D. Neilson, E. S. Orbesen, E. D. Prince, and J. R. Rooker. 2011. Evaluating post-release behaviour modification in large pelagic fish deployed with pop-up satellite archival tags. *ICES Journal of Marine Science* **68**:880-889.
- Horodysky, A. Z., D. W. K. R. J. Latour, and J. E. Graves. 2007. Habitat utilization and vertical movements of white marlin (*Tetrapturus albidus*) released from commercial and recreational fishing gears in the western North Atlantic Ocean: inferences from short duration pop-up archival satellite tags. *Fisheries Oceanography* **16**:240-256.
- Hussey, N. E., S. T. Kessel, K. Aarestrup, S. J. Cooke, P. D. Cowley, A. T. Fisk, R. G. Harcourt, K. N. Holland, S. J. Iverson, J. F. Kocik, J. E. Mills Flemming, and F. G. Whoriskey. 2015. Aquatic animal telemetry: A panoramic window into the underwater world. *Science* **348**:1255642.
- Ichinokawa, M., and J. Brodziak. 2010. Using adaptive area stratification to standardize catch rates with application to North Pacific swordfish (*Xiphias gladius*). *Fisheries Research* **106**:249-260.
- Lam, C. H., A. Nielsen, and J. R. Sibert. 2008. Improving light and temperature based geolocation by unscented Kalman filtering. *Fisheries Research* **91**:15-25.

- Lam, C. H., A. Nielsen, and J. R. Sibert. 2010. Incorporating sea-surface temperature to the light-based geolocation model TrackIt. *Marine Ecology Progress Series* **419**:71-84.
- Lam, C. H., B. Galuardi, and M. E. Lutcavage. 2014. Movements and oceanographic associations of bigeye tuna (*Thunnus obesus*) in the Northwest Atlantic. *Canadian Journal of Fisheries and Aquatic Sciences* **71**:1529-1543.
- Lin, S. J., M. K. Musyl, W. C. Chiang, S. P. Wang, N. J. Su, C. T. Chang, Q. X. Chang, Y. S. Ho, R. Kawabe, H. M. Yeh, and C. T. Tseng. 2020b. Vertical and horizontal movements of bigeye tuna (*Thunnus obesus*) in southeastern Taiwan. *Marine and Freshwater Behaviour and Physiology*. <https://doi.org/10.1080/10236244.2020.1852878>
- Lin, S. J., W. C. Chiang, M. K. Musyl, S. P. Wang, N. J. Su, Q. X. Chang, Y. S. Ho, I. Nakamura, C. T. Tseng, and R. Kawabe. 2020a. Movements and habitat use of dolphinfish (*Coryphaena hippurus*) in the East China Sea. *Sustainability* **12**:5793.
- Lu, C. P., C. A. Chen, C. F. Hui, T. D. Tzeng, and S. Y. Yeh. 2006. Population genetic structure of the swordfish, *Xiphias gladius* (Linnaeus, 1758), in the Indian Ocean and West Pacific inferred from the complete DNA sequence of the mitochondrial control region. *Zoological Studies* **45**:269-279.
- Madigan, D. J., A. J. Richardson, A. B. Carlisle, S. B. Weber, J. Brown, N. E. Hussey, and D. Secor. 2020. Water column structure defines vertical habitat of twelve pelagic predators in the South Atlantic. *ICES Journal of Marine Science*. <https://doi:10.1093/icesjms/fsaa222>
- Madigan, D. J., E. J. Brooks, M. E. Bond, J. Gelsleichter, L. A. Howey, D. L. Abercrombie, A. Brooks, and D. D. Chapman. 2015. Diet shift and site-fidelity of oceanic whitetip sharks *Carcharhinus longimanus* along the Great Bahama Bank. *Marine Ecology Progress Series* **529**:185-197.
- Madigan, D. J., W. C. Chiang, N. J. Wallsgrave, B. N. Popp, T. Kitagawa, C. A. Choy, J. Tallmon, N. Ahmed, N. S. Fisher, and C. L. Sun. 2016. Intrinsic tracers reveal recent foraging ecology of giant Pacific bluefin tuna at their primary spawning grounds *Marine Ecology Progress Series* **553**:253-266
- Matsumoto, T., T. Kitagawa, and S. Kimura. 2013. Vertical behavior of bigeye tuna (*Thunnus obesus*) in the northwestern Pacific Ocean based on archival tag data. *Fisheries Oceanography* **22**:234-246.
- Musyl, M. K., and E. L. Gilman. 2019. Meta-analysis of post-release fishing mortality in apex predatory pelagic sharks and white marlin. *Fish and Fisheries* **20**:466-500.
- Musyl, M. K., M. L. Domeier, N. Nasby-Lucas, R. W. Brill, L. M. McNaughton, J. Y. Swimmer, M. S. Lutcavage, S. G. Wilson, B. Galuardi, and J. B. Liddle. 2011b.

- Performance of pop-up satellite archival tags. *Marine Ecology Progress Series* **433**:1-28.
- Musyl, M. K., R. W. Brill, C. H. Boggs, D. S. Curran, T. K. Kazama, and M. P. Seki. 2003. Vertical movements of bigeye tuna (*Thunnus obesus*) associated with islands, buoys, and seamounts near the main Hawaiian Islands from archival tagging data. *Fisheries Oceanography* **12**:152-169.
- Musyl, M. K., R. W. Brill, D. S. Curran, N. M. Fragoso, L. M. McNaughton, A. Nielsen, B. S. Kikkawa, and C. D. Moyes. 2011a. Postrelease survival, vertical and horizontal movements, and thermal habitats of five species of pelagic sharks in the central Pacific Ocean. *Fishery Bulletin* **109**:341-368.
- Nakamura, I. 1985. FAO species catalog: billfishes of the world; an annotated and illustrated catalogue of marlins, sailfishes, spearfishes and swordfishes known to date. FAO Fisheries Synopsis.
- Palko, B. J., G. L. Beardsley, and W. J. Richards. 1981. Synopsis of the biology of the swordfish, *Xiphias gladius* Linnaeus NOAA Technical Report NMFS Circular 441 edition.
- Pekarsky, S., A. Angert, B. Haese, M. Werner, K. A. Hobson, R. Nathan, and D. M. Richardson. 2015. Enriching the isotopic toolbox for migratory connectivity analysis: a new approach for migratory species breeding in remote or unexplored areas. *Diversity and Distributions* **21**:416-427.
- Ramos-Cartelle, A., B. García-Cortés, I. González-González, A. Carroceda, J. Fernández-Costa, and J. Mejuto. 2018. A comparative review of size-weight relationships in north Atlantic swordfish (*Xiphias gladius*) based on records obtained in the Spanish surface longline fleet. *Collective Volume of Scientific Papers, ICCAT* **74**:841-967.
- Schaefer, K., D. Fuller, J. Hampton, S. Caillot, B. Leroy, and D. Itano. 2015. Movements, dispersion, and mixing of bigeye tuna (*Thunnus obesus*) tagged and released in the equatorial Central Pacific Ocean, with conventional and archival tags. *Fisheries Research* **161**:336-355.
- Sepulveda, C. A., A. Knight, N. Nasby-Lucas, and M. L. Domeier. 2010. Fine-scale movements of the swordfish *Xiphias gladius* in the Southern California Bight. *Fisheries Oceanography* **19**:279-289.
- Sims, D. W., E. J. Southall, G. A. Tarling, and J. D. Metcalfe. 2005. Habitat-specific normal and reverse diel vertical migration in the plankton-feeding basking shark. *Journal of Animal Ecology* **74**:755-761.
- Sims, D. W., E. J. Southall, N. E. Humphries, G. C. Hays, C. J. A. Bradshaw, J. W. Pitchford, A. James, M. Z. Ahmed, A. S. Brierley, M. A. Hindell, D. Morritt, M. K. Musyl, D. Righton, E. L. C. Shepard, V. J. Wearmouth, R. P. Wilson, M. J. Witt, and J. D. Metcalfe. 2008. Scaling laws of marine predator search

- behaviour. *Nature* **451**:1098-1102.
- Somiya, H., S. Takei, and I. Mitani. 2000. Guanine and its retinal distribution in the tapetum of the bigeye tuna, *thunnus obesus*. *Ichthyological Research* **47**:367-372.
- Sun, C. L., S. P. Wang, and S. Z. Yeh. 2002. Age and growth of the swordfish (*Xiphias gladius* L.) in the waters around Taiwan determined from anal-fin rays. *Fishery Bulletin* **100**:822-835.
- Thorrold, S. R., G. B. Skomal, J. Fontes, P. Afonso, P. Gaube, C. D. Braun, and D. Kaplan. 2019. Assimilating electronic tagging, oceanographic modelling, and fisheries data to estimate movements and connectivity of swordfish in the North Atlantic. *ICES Journal of Marine Science* **76**:2305-2317.
- Wang, S. P., C. L. Sun, and S. Z. Yeh. 2003. Sex ratios and sexual maturity of swordfish (*Xiphias gladius* L.) in the waters of Taiwan. *Zoological Studies* **42**:529-539.
- Wang, S. P., C. L. Sun, S. Z. Yeh, W. C. Chiang, N. J. Su, Y. J. Chang, and C. H. Liu. 2006. Length distributions, weight-length relationships, and sex ratios at lengths for the billfishes in Taiwan waters. *Bulletin of Marine Science* **79**:8750869.
- Zar, J. H. 2010. *Biostatistical Analysis*. Prentice Hall, New Jersey.
- Zhu, Q., K. A. Hobson, Q. Zhao, Y. Zhou, I. Damba, N. Batbayar, T. Natsagdorj, B. Davaasuren, A. Antonov, J. Guan, X. Wang, L. Fang, L. Cao, and A. David Fox. 2020. Migratory connectivity of Swan Geese based on species' distribution models, feather stable isotope assignment and satellite tracking. *Diversity and Distributions* **26**:944-957.

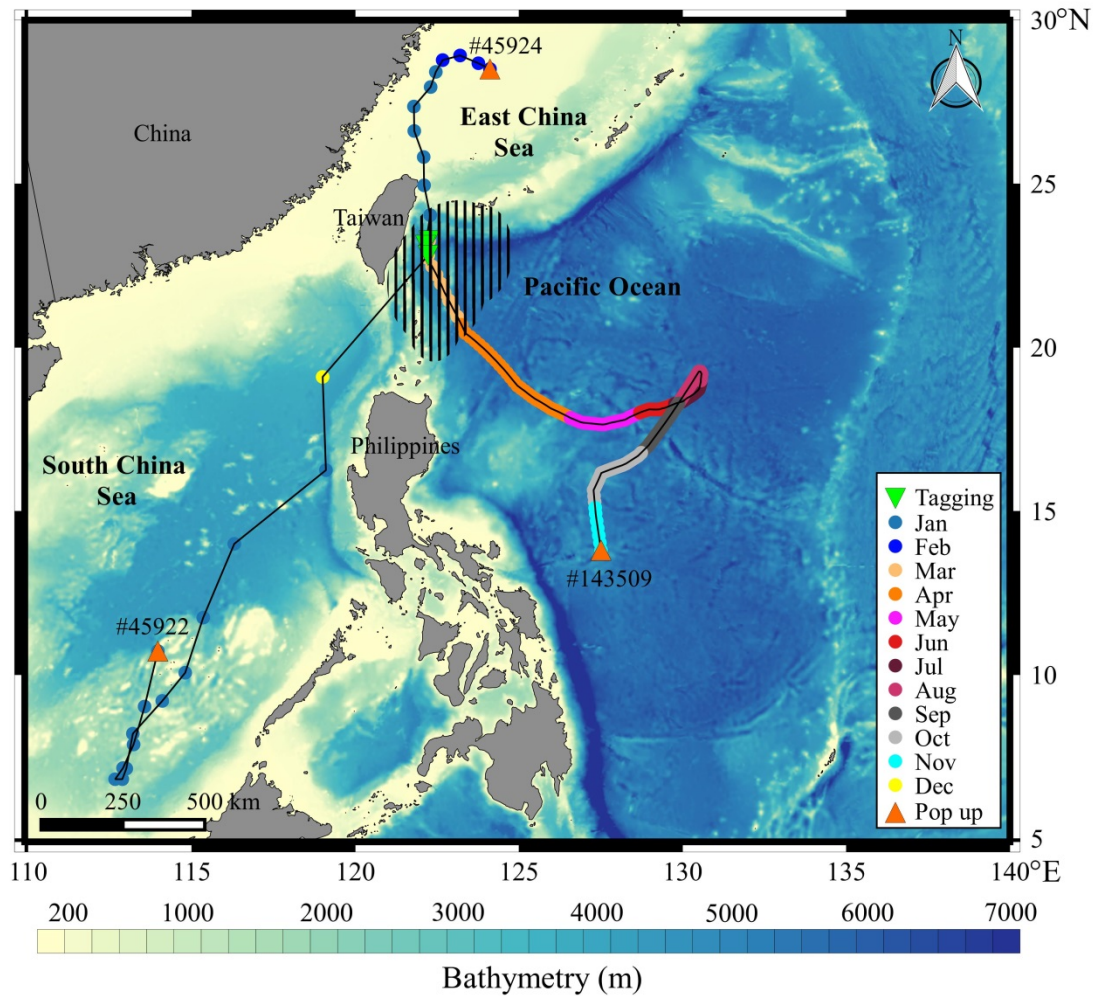


Fig. 1. Map of PSATs deployment on swordfish (triangles). Most probable tracks (circles and line) for all swordfish in different months are shown where pop-up location is depicted by stars. Fishing grounds of longline fishing operations based out of Shinkang fishing port in eastern Taiwan is shown in the hatched area.

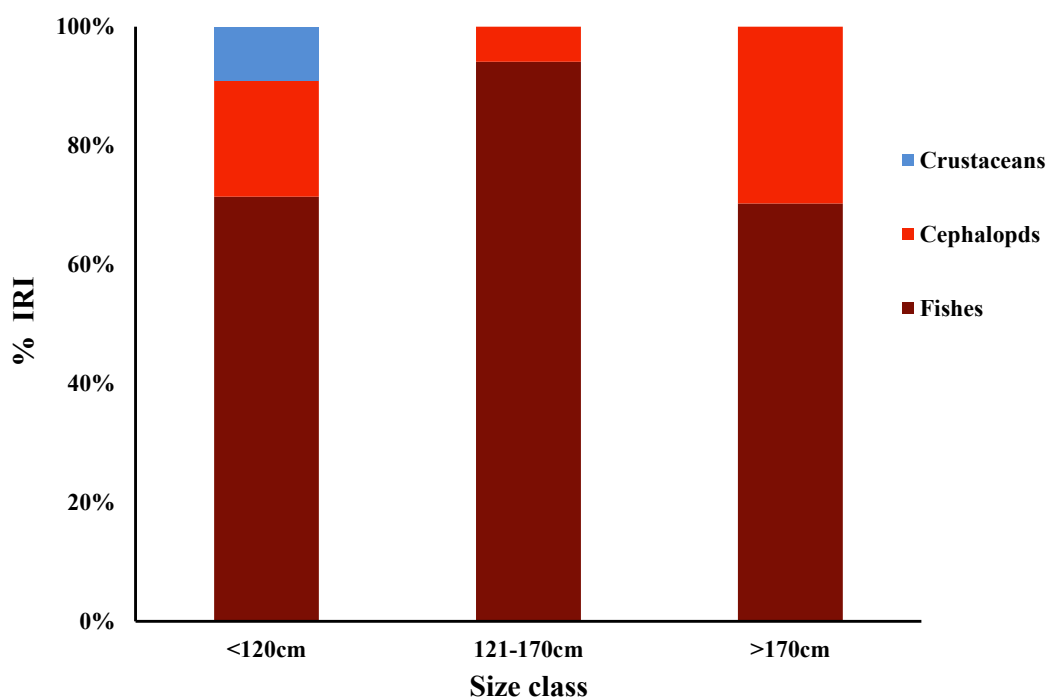


Fig. 2. Per cent index of relative importance (%IRI) by size class for the main prey species of swordfish caught off eastern Taiwan.

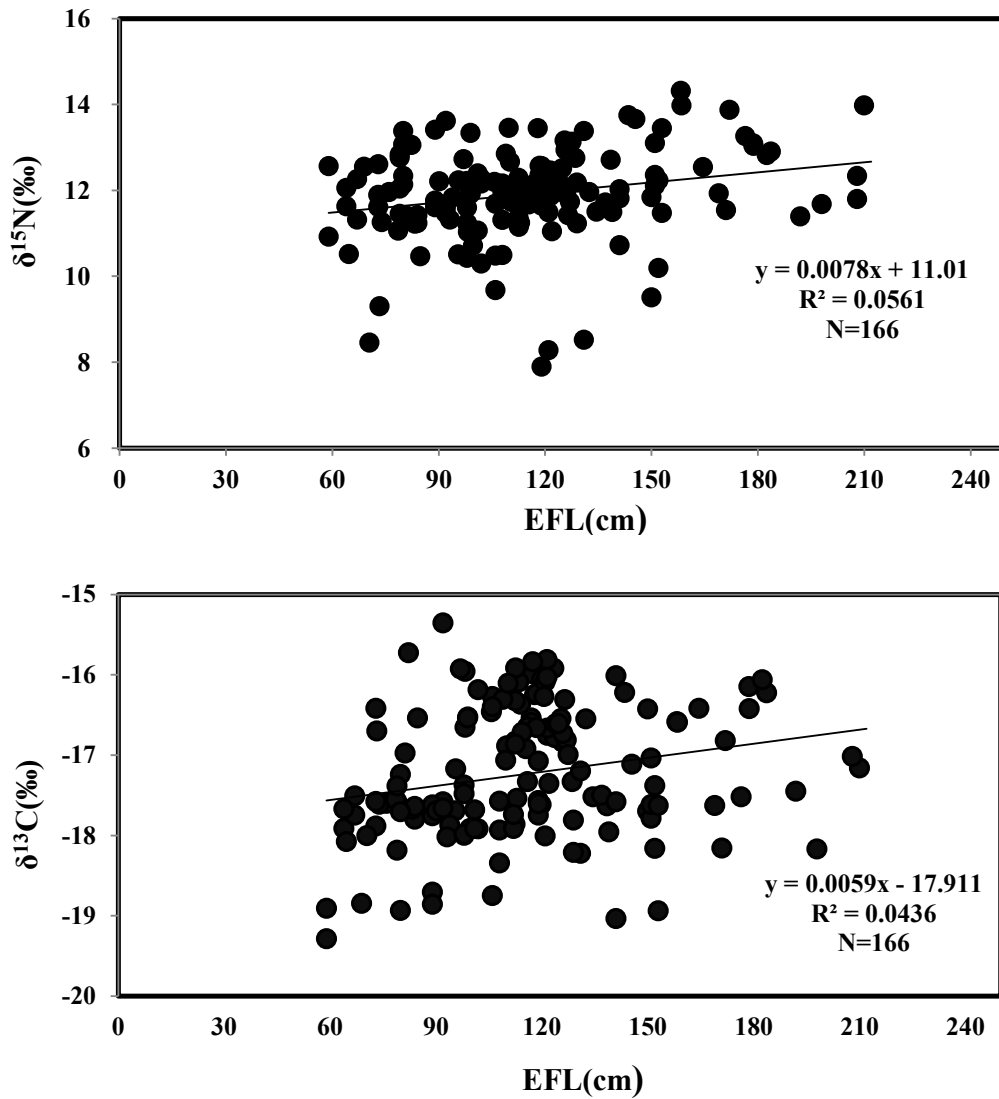


Fig. 3. The relationships of $\delta^{15}\text{N}$ (upper) and $\delta^{13}\text{C}$ values (lower) with eye-fork length (EFL) of swordfish off Taiwan.

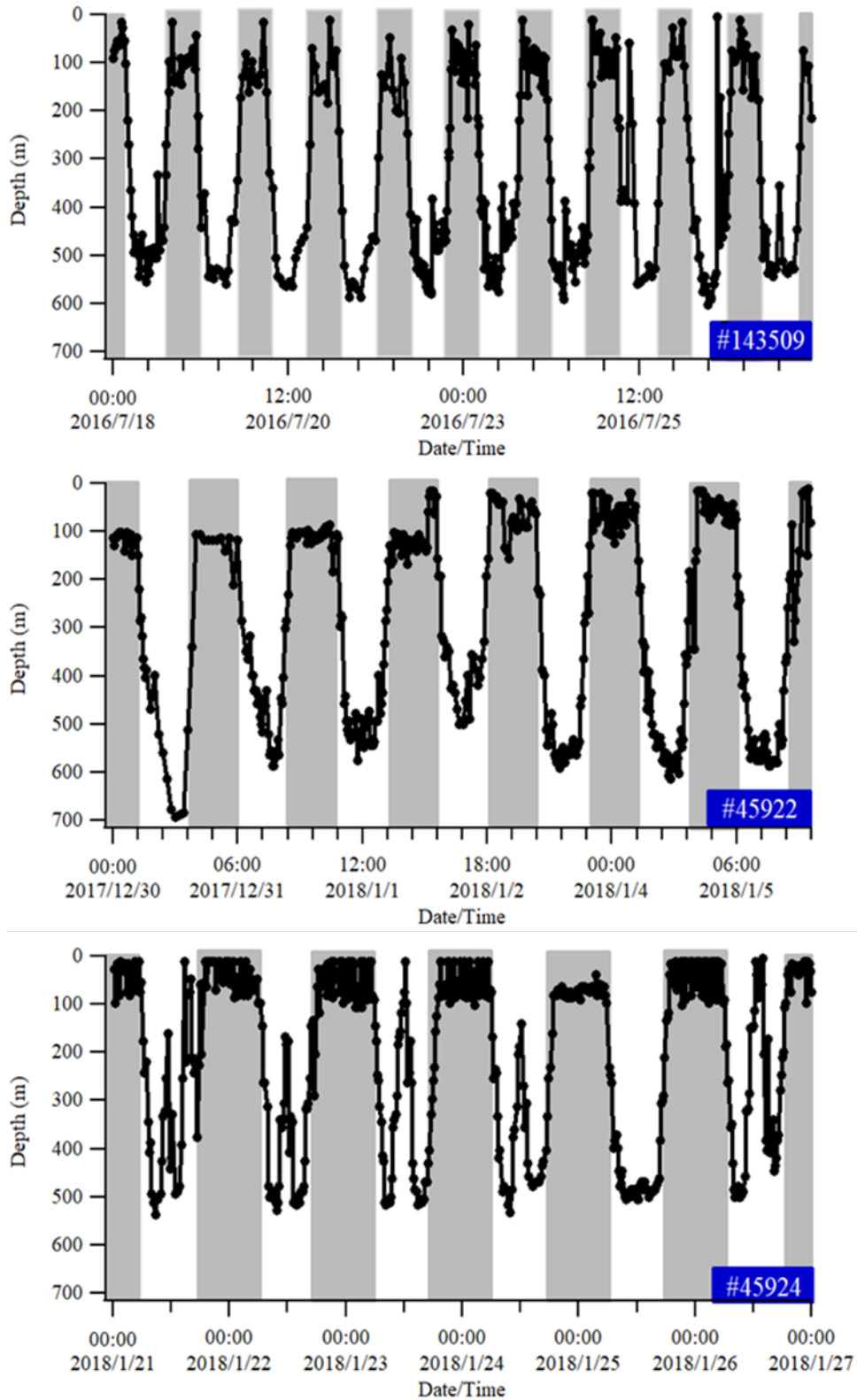


Fig. 4. Depth of diel vertical movements. Tagged numbers are provided. The gray vertical bars indicate nighttime.

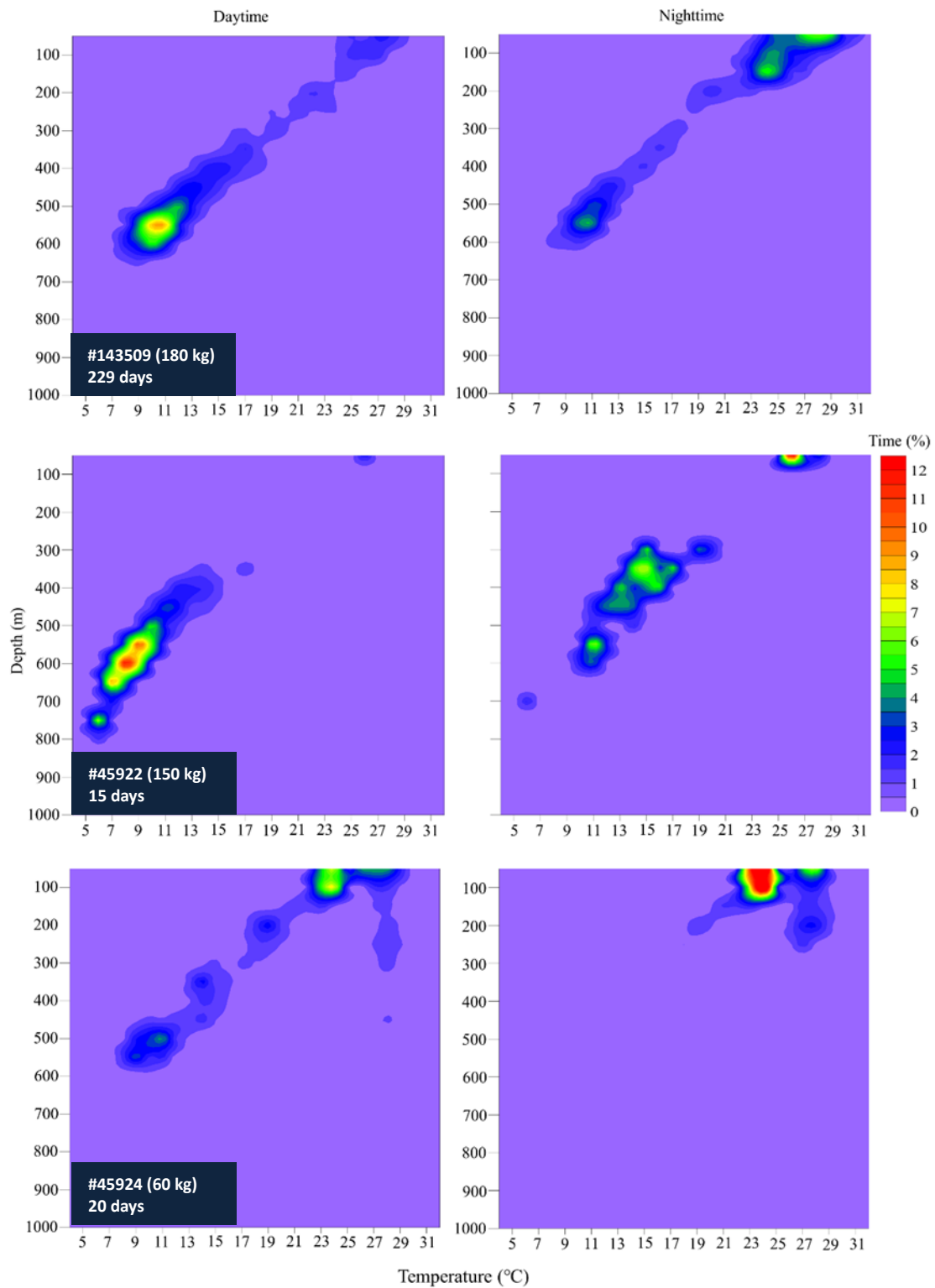


Fig. 5. Temperature-at-depth profiles showing the overall thermal utilization for three swordfish tagged with PSATs that were at liberty for 15–227 days.

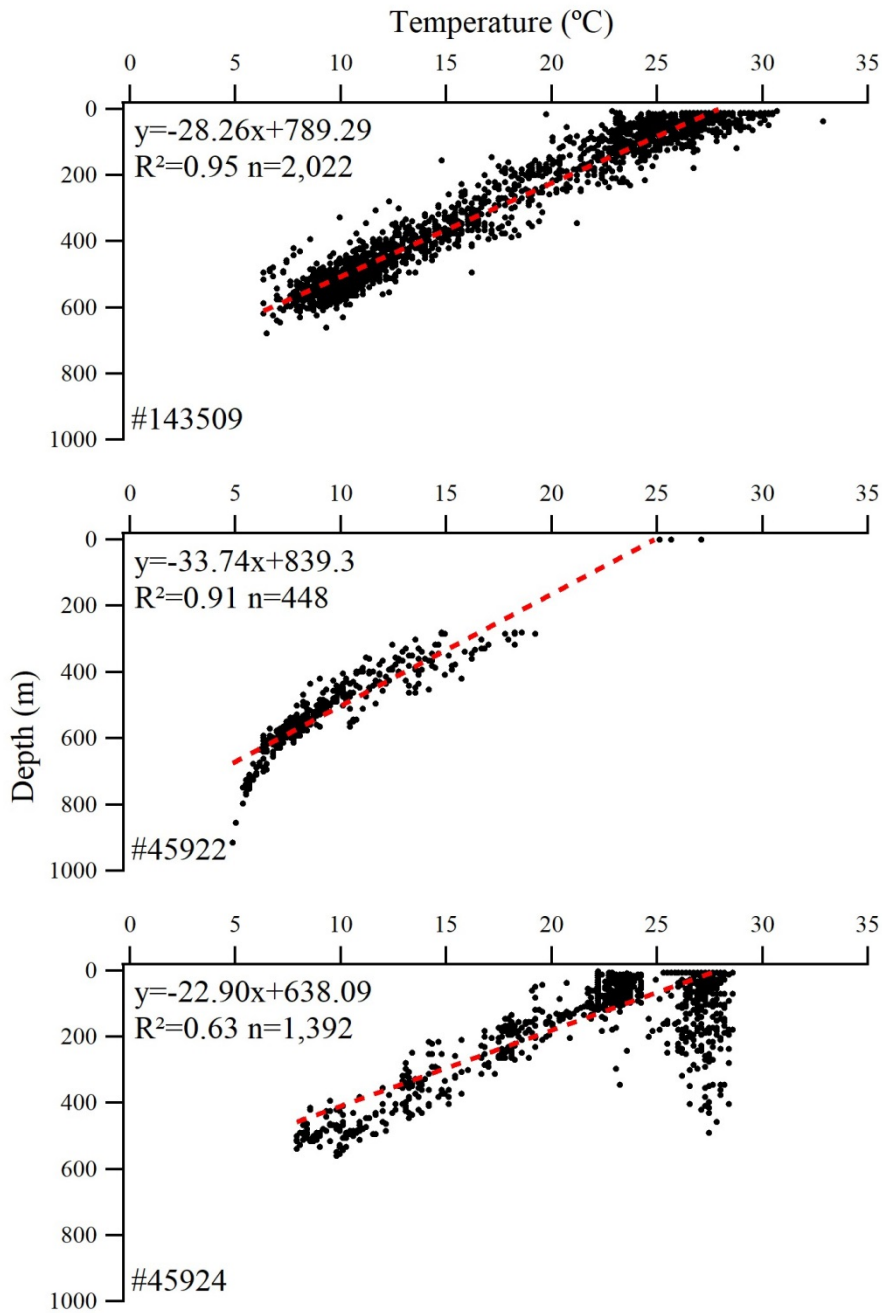


Fig. 6. Temperature-depth profile obtained from PSATs attached to swordfish. The red dashed lines are the fitted regression lines for the depth and temperature.

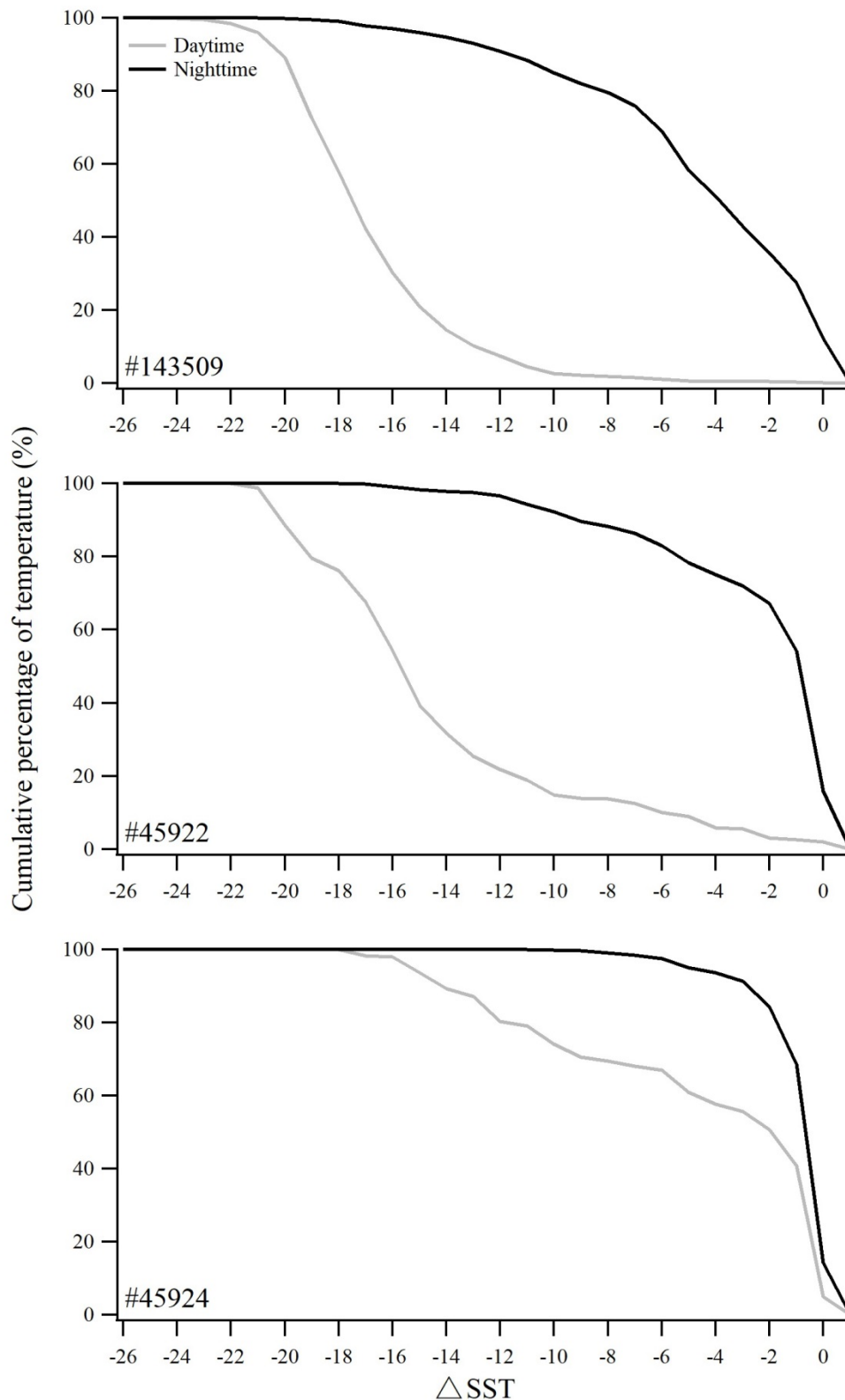


Fig. 7. Cumulative percentage of temperature readings from pop-up satellite archival tags (PSATs) attached to swordfish expressed as differences from daily mean sea surface temperature (Δ SST). SST was calculated as per Nielsen et al. (2006) and is analogous to Brill et al's (1993) surface layer.

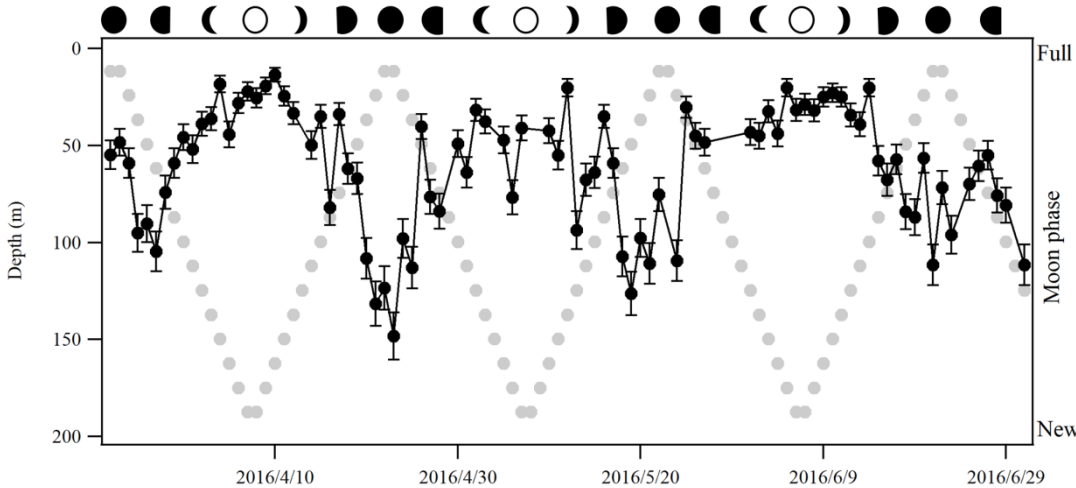


Fig. 8. Lunar illumination (dots) and nighttime mean (\pm SD) depth of SWO#143509.

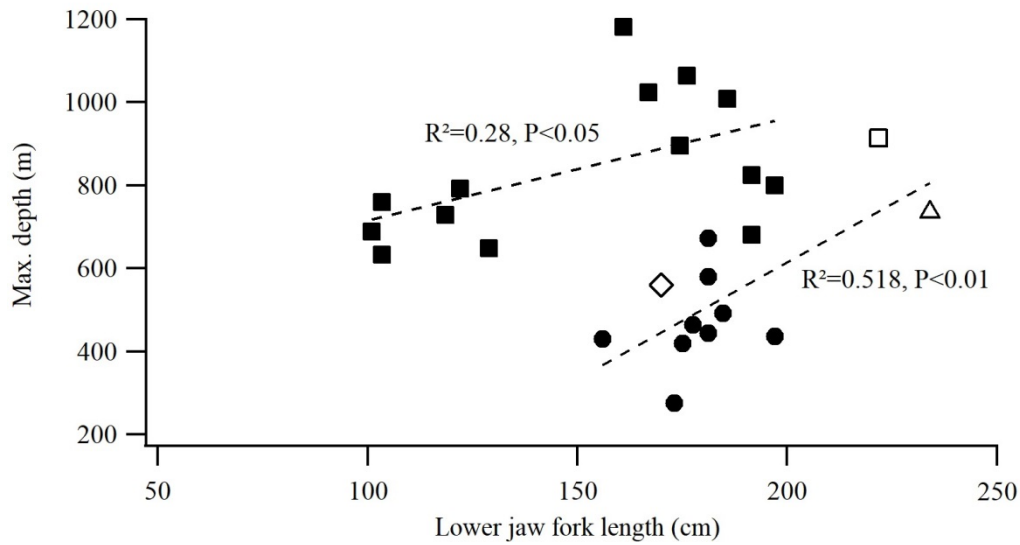


Fig. 9. For comparison, deepest dives of different sized tagged swordfish were obtained from electronic tagging studies. Symbols represent: present study (Northwestern Pacific Ocean for open triangle, South China Sea for open square and East China Sea for open diamond); (Sepulveda et al. 2010)(California for filled circle); (Thorrold et al. 2019) (North Atlantic for filled square). Estimated lower jaw fork length by (Ramos-Cartelle et al. 2018) and (Sun et al. 2002).

Table 1. The percentage in number (%N), frequency occurrence (%FO), percentage in weight (%W) and the %IRI of each prey species in swordfish stomachs.

Taxon	Number	%N	Frequency	%FO	Weight(g)	%W	%IRI
FISHES							
Bramidae. spp	19	7.45	19	37.25	11,304	32.63	23.30
Diretmidae. spp	2	0.78	1	1.96	1,002	2.89	0.11
Unidentified fish	180	70.59	18	35.29	6,485	18.72	49.19
CEPHALOPODS							
<i>Thysanoteuthis rhombus</i>	9	3.53	9	17.65	11,169	32.24	9.85
Unidentified Cephalopod	33	12.94	21	41.18	4,662.3	13.46	16.96
CRUSTACEANS							
Unidentified shrimp	12	4.71	4	7.84	13.46	0.05	0.58

Table 2. Values of $\delta^{15}\text{N}$ and $\delta^{13}\text{C}$ in different size classes of swordfish.

Samples	n	$\delta^{15}\text{N}$ (‰)				$\delta^{13}\text{C}$ (‰)			
		Mean	S.D.	Minimum	Maximum	Mean	S.D.	Minimum	Maximum
Class I (<120 cm)	101	11.7	0.9	7.9	13.6	-17.4	0.9	-19.3	-15.4
Class II (121-170 cm)	51	11.9	1.3	8.3	14.3	-17.2	0.8	-18.9	-15.8
Class III (>170 cm)	14	12.5	0.9	11.2	14.0	-17.1	0.7	-18.2	-16.1

Table 3. Details for pop-up satellite archival tags (PSATs) deployed on swordfish.

PSAT ID	Tagging date	PSAT version	Estimated weight (kg)	Days at liberty	Reporting date	Straight-line distance (km)
#143509	2016/3/23	PTT-100	180	229	2016/11/7	738
#45922	2017/12/27	X-tag	150	15	2018/1/10	1,605
#45924	2018/1/15	X-tag	60	20	2018/2/3	392

Table 4. Summary of the depth and temperatures obtained for pop-up satellite archival tags (PSATs) deployments on swordfish.

PSAT ID	Day depth (m)	Night depth (m)	Day temp. (°C)	Night temp. (°C)
	Min.-max. (mean±SD)	Min.-max. (mean±SD)	Min.-max. (mean±SD)	Min.-max. (mean±SD)
#143509	5.4-737	5.4-521	6.3-30.7	7-32.9
	477.7±92.9	114.5±105.6	11.3±2.7	23.5±4.4
#45922	0-914.5	0-677.8	4.9-25.1	5.8-27.1
	508.8±157.1	127.2±117.2	9.4±3.9	22.3±3.8
#45924	2.7-559.4	5.4-295.9	7.9-28.6	13.5-28.6
	156.5±177.8	65.1±57	19±6.6	24.1±2.4
Grand	0-914.5	0-677.8	4.9-30.7	5.8-32.9
Average	419.4±173.4	105.5±101.4	12.9±5.5	23.4±3.9